ATM Traffic Measurements and Analysis on a Real Testbed

S. Molnár[a], I. Cselényi[a], N. Björkman[b], C-G. Perntz[c], M. Boda[d]

[a]High Speed Networks Laboratory, Dept. of Telecom. and Telematics, TU Budapest
Sztoczek u. 2. H-1111 Budapest, Hungary, e-mail: {molnar,cselenyi}@ttt-atm.ttt.bme.hu

[b]Department of System Research, Telia Research AB
Rudsjöterrassen 2. S-13680 Haninge, Sweden, e-mail: nils.p.bjorkman@telia.se

[c]Switch Laboratory, Ericsson Radio AB,
Dialoggatan 1. S-12625 Kungens Kurva, Stockholm, e-mail:eracgp@kk.ericsson.se,

[d]Traffic Laboratory, Ericsson, Venyige u. 3. H-1103, Budapest, Hungary,
e-mail: ethmba@aristotel.eth.ericsson.se

Abstract This paper presents analysis results of multimedia traffic based on real measurements. The multimedia measurements have been carried out on the Stockholm Gigabit Network (SGN) where we used both CBR and 8 real VBR video sources. We have measured various characteristics of the real traffic like cell loss ratio, cell transfer delay, cell interarrival time etc. with different traffic conditions. The measurement data are used to analyze the traffic profiles as well as the impact of ATM multiplexer on these traffic traces. The measurements and analysis of traffic shaping is also carried out. The main contributions of the paper is to provide a comprehensive source characterization study as well as analysis results of multiplexing more real VBR video and CBR sources in a real ATM environment based on measurements.

1. Introduction

The evolution of multimedia communication services has opened various unresolved issues of traffic engineering ranging from the characterization of multimedia sources to the optimal dimensioning and control of ATM networks supporting a heterogeneous mix of multimedia traffic types [1, 2].

This wide range of challenges has yielded an enormous amount of research in recent years. In spite of the productive research work that has led to solutions to some of these problems, only a few comprehensive studies based on measurements of real ATM networks using the mix of actual VBR and CBR sources have been reported so far [3, 4]. However, efficient *traffic and congestion control* is impossible without the appropriate knowledge of the inherent nature of ATM traffic.

This paper presents analysis results of multimedia traffic based on real measurements. The measurements were carried out on the ATM testbed based on the Stockholm Gigabit Network (SGN, [5]) where a CBR stream was multiplexed with 8 real VBR video sources. The results obtained from these investigations are to be used in the Telia's commercial network, where there are numerous terminals and significant volume of network traffic.

Through our investigations, we can obtain a good understanding of the inherent nature of multimedia sources and traffic evolution in the network. The advantages with this study are summarized as follows. We have used a *wide-spread real ATM environment* rather than only lab trials, namely our testbed was the Stockholm Gigabit Network. Secondly, we have used *real multimedia sources* avoiding the use of any artificially generated VBR traffic. Thirdly, *a relative large amount of real sources* were used in our experiments providing the opportunity to observe the multiplexing effects on these sources. Finally, our measurements were carried out with a *high resolution ATM test tool* developed in the RACE PARASOL project that provided advanced measuring facilities not available in commercial ATM measurement instruments.

The paper organized as follows. Section 2 describes our network scenario and environments as well as the measuring tools. The description of our test cases are presented in Section 3. Results concerning the cell loss process and cell transfer delay with our shaping study are reported in Section 4. In the next section we give both a source characterization and multiplexing effect study. Finally concluding remarks are in Section 6.

2. Measurements of Multimedia Traffic

2.1 Network Environment

The measurements were made on a typical topology of an ATM campus network where the traffic sources are concentrated in each site by means of ATM multiplexers before getting into the large area public network. The network scenario was realized on a spatially distributed MAN environment, namely on the *Stockholm Gigabit Network* [5]. This network based on a 622 Mbps, optical double ring connecting seven research and development sites throughout Stockholm over 110 km. Two of these sites, Telia Research (TRAB) in Haninge and Ericsson UA (EUA) in Älvsjö with a distance of about 25 km from each other, were involved in our experiments. Four multimedia workstations and an ATM node was situated in Älvsjö and the rest of instruments in Haninge as shown in Fig. 1.

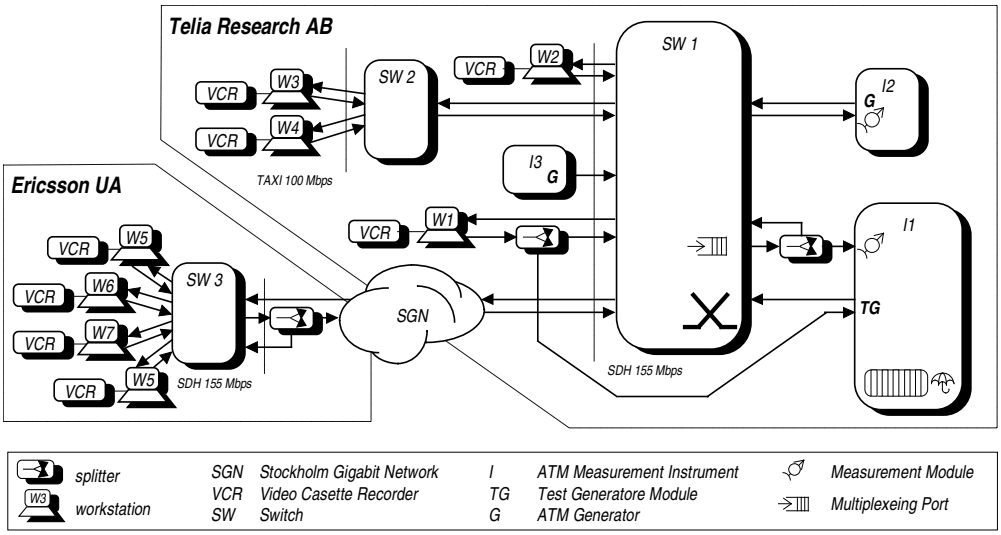

Fig. 1. Measurement Environment

The switches *SW1-SW3* acted as multiplexers, instrument *I3* as a CBR traffic source and the eight workstations, *W1-W8* as VBR traffic sources. The aggregate traffic streams from the concentrator switches together with the CBR traffic stream were directed into the same port of an ATM backbone switch, i.e. into a common multiplexer.

2.2 Traffic Sources

Variable Bit Rate Video Sources

Eighth workstations equipped with video, audio hardware and ATM network interface cards were applied as VBR traffic sources. Since a repeatable input video source was required, a video cassette recorder was connected to each multimedia workstation. Video conference applications (ShowMe [6], vic [7]) were started between pairs of multimedia workstations (*W1-W2*, *W3-W4*, ..) communicating through PVC ATM connections. The features of sources, such as name of video sequences, type of ATM network interface cards and workstations, long term average cell rates are presented in Table 1. Various setting combinations of these features were investigated, but only a fraction of them is reported in this paper.

Constant Bit Rate Source

Two commercially available instruments (*I2* and *I3*) were used to generate background CBR traffic in the test case (a), (b) and (c), alternately. The applied CBR rates are reported in the description of test cases in Chapter 3.

2.3 ATM Multiplexers, Nodes

ATM departmental switches were applied for concentrating the traffic of VBR sources in both sites. In order to avoid cell loss at EUA site, a shaping rate of 35 Mbps was applied in each workstations. It did not changed the main characteristics of VBR streams since the average rate was much lower. Each switch had a FIFO like multiplexing service and neither cell prioritization nor policing was applied. The physical interface types of switches are denoted in Fig. 1.

2.4 Measurement Instruments

ATM traffic characteristics were measured by two different ATM measurement instruments (I1, I2). The arrival time of ATM cells of interest was recorded in real-time by a module developed by Telia AB, Sweden. It resides in an ATM test instrument (I1) developed in the RACE PARASOL project. This instrument is capable of recording about 8 million cell arrivals [18]. The traffic records were analyzed with a Telia proprietary software program. The cell flow could be visualized in any level of detail, ranging from individual cells to full recordings of several hours. For the statistical analysis, some extension software made by the authors were used. An other module of I1 instrument was used for replacing the ATM cell stream with test cells, containing timestamp and sequence number. This way cell loss and cell transfer delay could be captured for longer periods up to several hours. HP Broadband Test Series 7500 Instrument (I2) and an HP 37717C (I3) were used to generate CBR traffic and to collect statistical traffic characteristics like average and variance of Cell Interarrival Time (CIT) or Cell Transfer Delay (CTD).

Source	Video Sequence	Application, Compression	QoS Performance Setting	Platform	ATM Network Interface Cards	Shaping Rates [Mbps] 1.	2.	Long term Traffic Average [kbps]
W1	Star Wars 1	ShowMe CellB	PAL 768x576, 10 fps	SunSPARC 10	Fore SBA 200 SDH	-	12.5	3612
W2	Star Wars 2	ShowMe CellB	PAL 768x576, 10 fps	SunSPARC 10	Fore SBA 200E SDH	-	12.5	3640
W3	Die Hard	vic CellB	PAL 768x576, 10 fps	Silicon Graph-ics Indigo	Fore SBA 200E TAXI	-	12.5	3901
W4	Wily Free	vic CellB	PAL 768x576, 10 fps	SunSPARC 10	Fore SBA 200E TAXI	-	12.5	3689
W5	Terminator 1	ShowMe CellB	PAL 768x576, 10 fps	SunSPARC 20	SAHI-2 SDH	35	4	3600
W6	Green Card	ShowMe CellB	PAL 768x576, 10 fps	SunSPARC 20	SAHI-2 SDH	35	4	3738
W7	Terminator 2	ShowMe CellB	PAL 768x576, 10 fps	SunSPARC 10	SAHI-2 SDH	35	4	3450
W8	Fish Called Wanda	ShowMe CellB	PAL 768x576, 10 fps	SunSPARC 10	Interphase SDH	35	8	3259

Table 1. Features of VBR Sources

3. Test Cases

The measurement set-up depicted in Fig. 1 was used for investigations. Test cases for (a) long-time cell loss and cell delay measurement, (b) traffic source analysis, (c) investigation of multiplexing effect and (d) shaping were based on this general scenario.

The optical signal from VBR source (*W1*) was tapped to the ATM test equipment by means of an optical splitter. In this way we captured an exact copy of the cell flow between terminals without disturbing the application. An other splitter was placed after the multiplexer

collecting the whole aggregate ATM traffic, in order to make a copy of cell stream for measurement module of instrument *I1*.

a) Cell-loss and cell transfer delay

All devices depicted in Fig. 1 were involved in this test case. The ATM cell stream generated by a VBR traffic source *W1* was duplicated by an optical splitter. One of these cell streams was directed to workstation *W2* through the switch *SW1* without going through the multiplexing port. The other cell stream was forwarded to the test equipment *I1*. The cells of this stream were replaced with test cells containing time stamps and sequence number by *I1* and fed to the multiplexer of *SW1*. In this way an exact copy of the original cell stream between terminals was captured and replaced with test cells without effecting the behavior of the application in use. After the multiplexing port, the aggregate traffic was splitted into two parts. One part was directed back to the appropriate workstations and the other was fed into the analyzer module of *I1* instrument.

The CBR background load was increased in three steps; 80.136 Mbps, 101.336 Mbps and 122.536 Mbps. Cell loss process and cell transfer delay of *W1* traffic were measured by *I1* for half an hour long records. The multimedia application on the workstations and the video tapes were started according to the same scheduling.

b) Source Characterization

The ATM traffic stream from every single workstations, separately, was directed into the *I1* instrument in order to capture the entire cell arrival process for analysis. Beyond the goal of understanding the traffic structure the purpose of this source characterization was to estimate the proper background load values and shaping rates.

c) Investigation of ATM Multiplexing

ATM traffic streams from VBR sources *W1*, *W2* and the CBR traffic from *I2* were multiplexed in *SW1*. Statistics of CBR source, such as minimum, mean, maximum and variance, of cell interarrival time and cell transfer delay were calculated from several thousands captured cell arrival by *I2* which generated cells containing timestamps for this goal. The whole cell arrival process for CBR and VBR sources was captured by *I1*. CBR load spanned through the link from 10 to 140 Mbps with steps 10 Mbps. According to the results of source characterization [16, 17], the intensity of video sequence has an impact on traffic characteristics. That is why a high average rate (5470 kbps) *quasi white-noise* input video was used in *W1* and *W2* in order to get worst case statistics. The length of the recorded VBR and CBR cell stream were 20 sec and 4 sec, respectively.

d) Investigation of Shaping

Two sets of shaping rates were applied in the measurements shown in Table 1. The shaping setting 1 practically considers the case when the sources are not shaped (only 4 sources at EUA were shaped to 35 Mbps). The shaping setting 2 represents a mix of heterogeneous shaping rates as set by the users of the workstations. The effect of shaping on Cell Loss Ratio and Cell Transfer Delay were examined.

4. Analysis of Cell Loss and Delay

According to Fig. 1 and the description of test case (a) and (d), the aggregate traffic of four workstations in EUA (*W5-W8*) were multiplexed in *SW2* and fed to the optical ring of SGN toward TRAB. The traffic of workstations *W2-W4*, the CBR source *I3*, test cells cor-

responding to the cell stream from *W1* and the aggregate traffic from EUA were directed into the same port of *SW1*. Therefore, eighth VBR and a CBR sources were involved in this measurements.

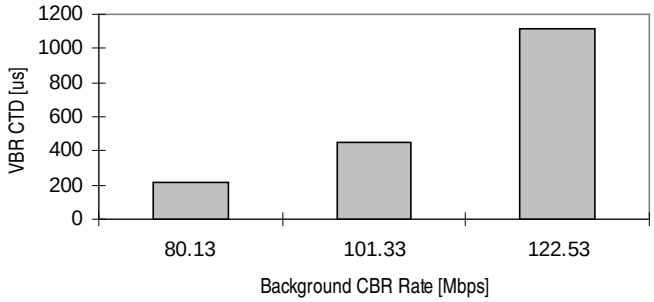

Fig. 2. Cell Transfer Delay of a VBR Traffic as a Function of CBR Background Rate

The cell transfer delay and the long term cell loss ratio were measured on the test cell stream in case of different background CBR load as shown in Fig. 2 and Fig. 3, respectively. The results of the cell transfer delay show that how the additional delay caused by queuing in the multiplexing buffer increases if we increase the CBR background load. The results related to the extremely large load was tested in order to get a view about how drastically the cell transfer delay and cell loss can increase.

The link utilization was also investigated. The cell loss ratio for the shaped and non-shaped cases are depicted in Fig. 3. From this Figure we can see how much bandwidth can be gained by using shaping with keeping an acceptable video quality. For example at the 10^{-5} cell loss level, which is considered for Class 2 in [11], we can gain approximately 25 Mbps bandwidth by shaping.

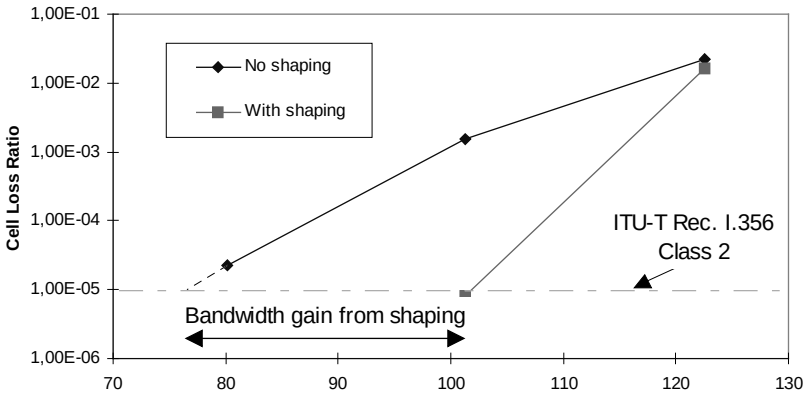

Fig. 3. Cell Loss Ratio of a VBR Traffic as a Function of CBR Background Rate

The application of shaping can allow us to achieve better link utilization as shown in Table 2. In our example ATM traffic shaping improved the link utilization form 71% to 88%. The example also demonstrates that statistical multiplexing was possible both with and without shaping. With shaping 46.73 Mbps bandwidth was used for the 8 VBR video sources instead of 70 Mbps (the sum of shaped source rates, see Table 1) which would be the case of peak rate allocation.

	Total link capacity	CBR background load	Equivalent bandwidth of 8 VBR sources	Utilization of total link capacity
Rate 1 (no shaping)	149.76 Mbps	77.59 Mbps	72.71 Mbps	71 %
Rate 2 (shaped sources)	149.76 Mbps	103.03 Mbps	46.73 Mbps	88 %

Table 2. The Impact of Shaping on the Link Utilization

5. Source Characterization and The Effect of Multiplexing

The goal of the study presented in this Section is twofold. The VBR and CBR cell stream statistics are analyzed both before the multiplexer, which gives us the source characteristics, and also after the multiplexer, which help us to understand the multiplexing effect. For this analysis we used the test case (b) and (c), respectively.

5.1 CBR Traffic Characteristics

The Constant Bit Rate (CBR) services are currently seen as one of the relevant ATM applications which coexists with VBR services [8, 9]. This traffic arises e.g. from CBR video coders or circuit emulation. The generated CBR traffic can sufficiently be characterized by its peak rate. However, the original CBR traffic may get distorted as it is traveling through the network due to the interference by other traffic streams in ATM multiplexers. This distortion phenomenon of cell streams is described by *Cell Delay Variation* (CDV) which has been intensively investigated by both ITU and ATM Forum [9, 10, 11] and one of the most important performance measure of CBR traffic. The analysis of CDV has been the main subject of a number of recent studies including both analytical models and simulation methods [12, 13, 14, 15]. However, a few results of CDV affected CBR cell streams based on measurements are reported so far, specially when the background traffic in the ATM multiplexer is generated by real sources. We provide such an analysis in this Section.

A critical impact of CDV on CBR cell streams is the *clumping effect* when the interarrival times between consecutive cells of a connection is less than the period of the CBR cell stream, i.e. the temporary cell rate is larger than the CBR rate. This phenomenon causes significant difficulties to the peak cell rate control mechanism located in the UPC/NPC. We have analyzed the clumping effect by displaying the cumulative probability distribution function of the CBR cell interdeparture time (measured after the multiplexer) shown in Fig. 4. In our case this effect is even more difficult to investigate since the rate of CBR source is high compared to the link rate, i.e. the discrete nature of ATM plays a dominant rule. Therefore, between 75 Mbps and 150 Mbps the CBR period is between 2 and 1 and not an integer multiples of the cell time. It causes the effect that e.g. a 100 Mbps CBR cell stream (without CDV) puts 2 cells out of 3 time slots (if, for simplicity, the disturbing effect caused by the management cells and also the effect that the period of 100 Mbps cell stream is not exactly an integer multiplier of the 2/3 slot time of the carrier slot are neglected). It means that the 100 Mbps CBR cell stream has the structure that two cells arrive back-to-back following an empty cell slot yielding to a probability mass function of the interarrival time with 0.5 value at both 1 and 2 cell times (Fig. 6). From the Fig. 4 we can observe that the number of back-to-back cells increased by approximately 10% (0.55) in case of the CDV affected 100 Mbps CBR cell stream due to the clumping effect.

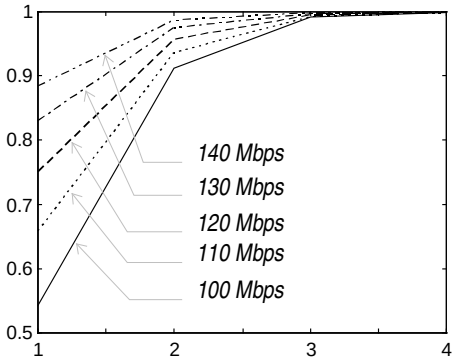

Fig. 4. Cumulative Distribution Function of CDV Affected CBR Cell Streams

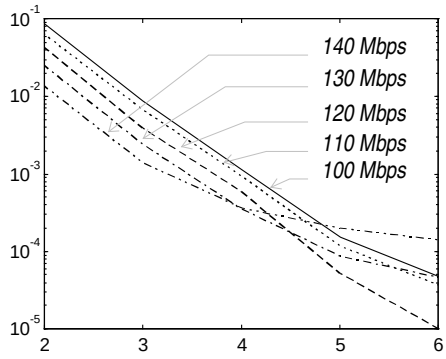

Fig. 5. Complementary Distribution Function of CDV Affected CBR Cell Streams

The opposite effect of cell clumping is the *cell dispersion* when the interarrival times between consecutive CBR cells is larger than the CBR period. It means that we can observe gaps between cells of a CBR connection. The cell dispersion causes problems for the AAL and the user terminal because they are usually sensitive to cell gaps. They have the functionality to restore the original periodic structure of CBR cell streams but e.g. cell gaps may interrupt the cell disassembling process. The dispersion effect can be well investigated by observing the complementary distribution function of the CBR cell interdeparture time (measured after the multiplexer) shown in Fig. 5. It can be seen that for all investigated CBR cell stream significant cell dispersion occurred, e.g. in the case of 100 Mbps CBR cell stream the probability of having cell interarrival time more then 3 time slots is more then 10^{-2}.

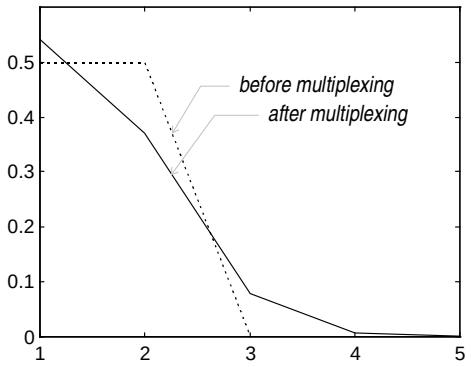

Fig. 6. Probability Mass Function of the Interarrival and Interdeparture Time of the 100 Mbps CBR Cell Stream

To show how the CBR cell stream profile has been changed going through the multiplexer we plot the probability mass function of the 100 Mbps CBR cell interarrival and interdeparture time in Fig. 6. We can see both the clumping and dispersion effect in this Figure.

The probability mass function of the CBR cell interdeparture time measured at the output of the multiplexer is shown for different CBR load in Fig. 7. We can observe that the higher the CBR rate the smaller the absolute CDV (the deviation from the expected value of the interdeparture time). It can be explained by noting that these high rate CBR cells arriving in

full rate bursts (e.g. for 100 Mbps CBR two cells, for 120 Mbps CBR four cells, for 130 Mbps CBR six cells arriving in a full rate burst followed by an empty time slot) and multiplexing them with the interfering VBR cell streams result in cell streams where the number of consecutive CBR cells having several time slots distance in between decreases as we increase the CBR rate. In Fig. 8 the same distributions are plotted in the function of the relative CDV, i.e. the ratio of cell interdeparture time to the CBR period, therefore the effect caused by changing the CBR cell rate can be covered here.

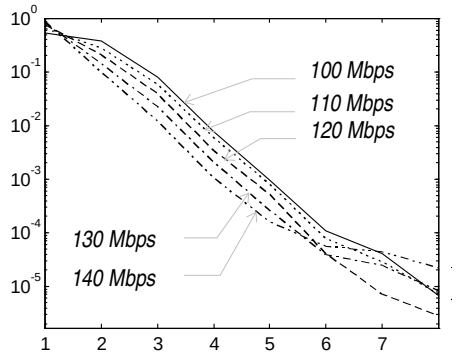

Fig. 7. Probability Mass Function of the CBR Cell Interdeparture Time

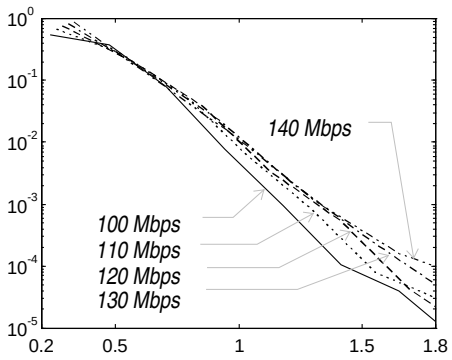

Fig. 8. Probability Mass Function of the Relative CDV

We have also analyzed the CDV effect by investigating the peak-to-peak CDV suggested by the ATM Forum [10]. We considered the peak-to-peak CDV related to the zero quantile, i.e. the difference between the minimum and maximum cell transfer delay. The peak-to-peak CDV as a function of the CBR load is depicted in Fig. 9. As can be seen from Fig. 9 the peak-to-peak CDV linearly increases as the CBR rate increases showing the increasing queuing time in the multiplexing buffer.

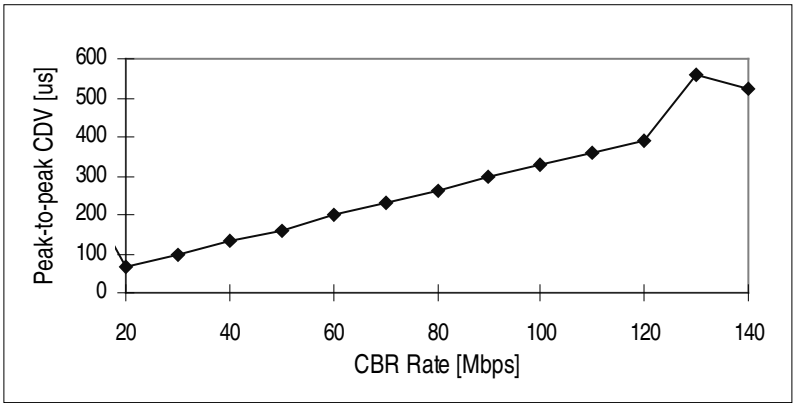

Fig. 9. Peak-to-peak CDV of CBR Cell Stream After the Multiplexer

The burstiness of the CDV affected CBR cell stream is also investigated. We used the squared coefficient of variation of the cell interdeparture time as a measure of burstiness. The results are plotted in Fig. 10.

Here two phenomenon have effects on the burstiness. On one hand the discrete nature of ATM plays a dominant rule, namely, the pure CBR cell stream (without CDV) deviates from the theoretical CBR stream, i.e. it has *inherent burstiness* due to the fact that the cell interarrival time is not constant. This burstiness of the CBR stream is plotted in the Figure. On the other hand some burstiness can be detected due to the interfering VBR cell streams (the CDV effect).

As we can see in some range of the high rate CBR streams that the inherent burstiness of the CBR becomes dominant in the total burstiness which was measured after the multiplexer. In case of low multiplexing load we have the increasing burstiness vs. load curve as we could expect. However, it is interesting to see that for increasing further the load (above 0.7) the total burstiness is decreasing. It can be explained by noting that in the investigated range the dominating CBR cell stream have more and more back-to-back cells if we increase the CBR load, i.e. no space for dispersion.

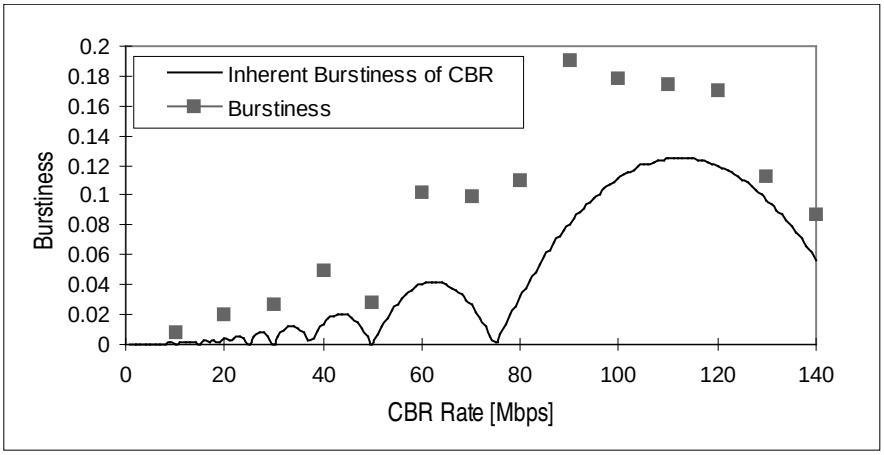

Fig. 10. The Squared Coefficient of Variation of CBR Cell Interdeparture Time

This results can be used also for setting up models for the perturbed CBR cell stream. As an example in the literature more results are reported using the renewal process as an approximation for the CDV affected CBR cell stream [12] where the important characteristics which should be matched is the squared coefficient of variation of the cell interarrival time and it can be read from this Figure.

We analyzed the Index of Dispersion for Intervals (IDI) [19] of the CDV affected CBR cell stream. The IDI is found to be a very useful tool to describe point processes which gives a complete second order characterization of the investigated cell process. The IDI curves of a 100 Mbps CBR cell stream before and after the multiplexer are shown in Fig. 11. The CBR cell stream has negative correlation before the multiplexer due to the periodic structure which clearly displayed by the decreasing IDI curve. This structure is destroyed by multiplexing the CBR cell stream with the two bursty VBR cell streams and positive correlation is detected by the increasing IDI curve. The explanation of this phenomenon is that because of the well-filled structure of such a high rate CBR cell stream remarkable dispersion cannot occur but

there is a tendency for significant cell clumping. Therefore the burstiness of the high rate CBR cell stream increases after the multiplexing. However, this process is still smoother than the Poisson process.

The IDI is plotted for different CBR rates in Fig. 12. As we can see the correlation structures of all the investigated CBR cell streams after the multiplexing are almost the same. This structure is dominantly determined by the traffic profile of the interfering VBR cell streams discussed in the next Section.

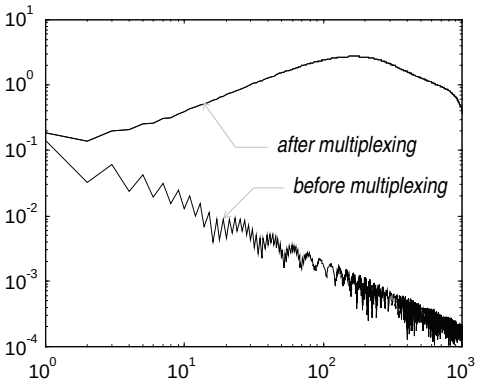

Fig. 11. Index of Dispersions for Intervals of 100 Mbps CBR Cell Streams

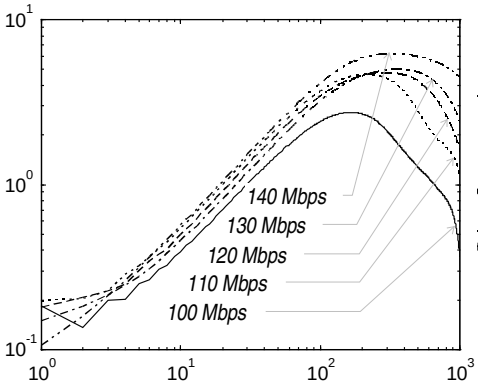

Fig. 12. Index of Dispersions for Intervals of CBR Cell Streams

5.2 VBR Traffic Characteristics

The Variable Bit Rate (VBR) services [10] cover a broad range of required ATM applications. VBR traffic arises both in data communication like LAN interconnection and also video communication like real-time video conferencing. The VBR traffic has rather complex structure and it is described by additional two source traffic descriptors: the sustainable cell rate with the maximum burst size beside the peak cell rate [9, 10].

The VBR cell stream before the multiplexer has been recorded for source characterization. The traffic intensity variation of the VBR video sequence is depicted in different time scales ranging from *sec* to μs in Fig. 13-16. A 20 sec measurement period of the video trace is depicted in Fig. 13. It can be observed that there is no pronounced high and low traffic segments of the trace but rather it shows almost the same average load with the same structure. It is due to the fact that the content information is noise-type therefore the video coder generates frames with almost the same statistics. 6 video frames have been zoomed out from this figure and presented in Fig. 14. The compression efficiency of the video coder is low because of the noise-type content (test case c) and it resulted in large frames during the whole trace. The deterministic property of the video sequence is well observable in this Figure. Zooming out a video frame the packet structure can be observed in Fig. 15. The frame consists of 9 and a half packets with a deterministic structure. Finally going to cell scale we find 180 almost consecutive cells in a video packet as shown in Fig. 16.

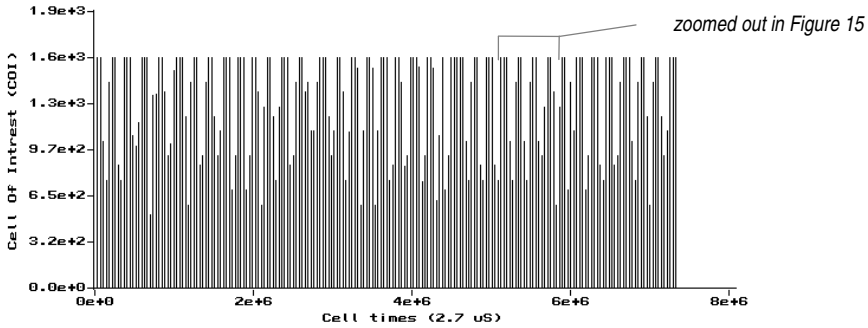

Fig. 13. VBR Video Burst Level
(window length: 20 sec, average rate in the window: 5.56 Mbps)

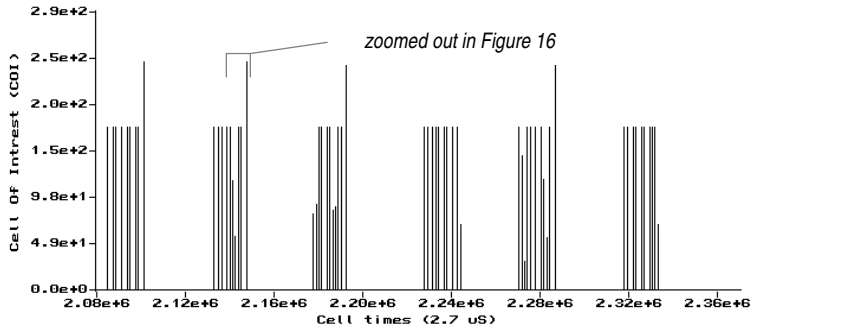

Fig. 14. VBR Video Frame Level
(window length: 760 ms, average rate in the window: 6 Mbps)

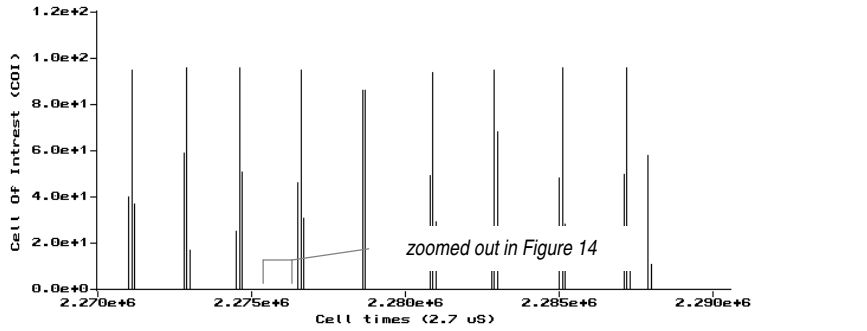

Fig. 15. VBR Video Packet Level
(window length: 50 ms, average rate in the window: 12.5 Mbps)

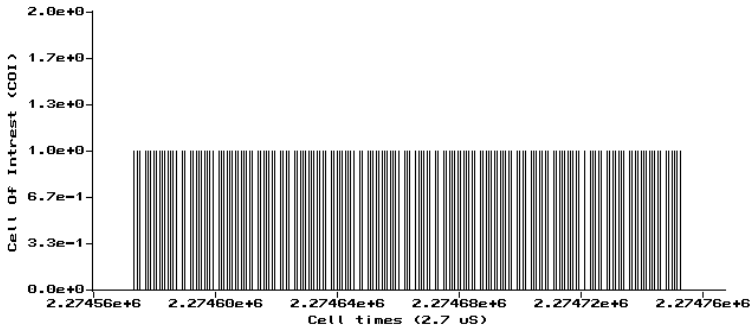

Fig. 16. VBR Video Cell Level
(window length: 54.5 μs, average rate in the window: 144.7 Mbps)

We can analyze the multiplexing effect on the VBR cell stream by plotting the probability mass function of the VBR cell interarrival and interdeparture time measured at the input and output of the multiplexer, respectively. In Fig. 17 these curves are shown where the probability mass function of the VBR cell interdeparture time are also depicted for different CBR load. The range of 1 to 10 cell times are shown because the main probability mass is concentrated in this range.

The results clearly show that the original structure of VBR traffic, which is basically built on bursts with back-to-back cells, have been destroyed and the dispersion of VBR cells become more and more significant as we increase the CBR load.

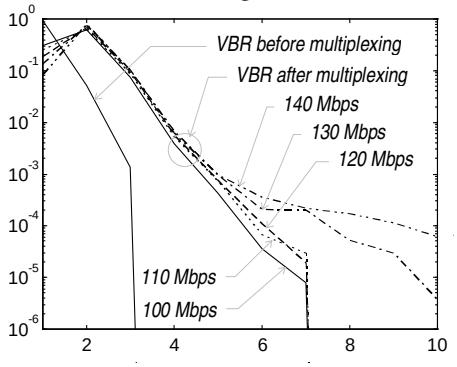

Fig. 17. Probability Mass Function of VBR Interarrival and Departure Time

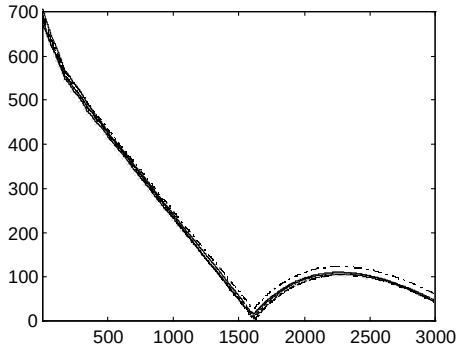

Fig. 18. Index of Dispersions for Intervals of VBR Video Streams

The IDI of the VBR cell streams before and after the multiplexer were calculated for the different CBR interfering traffic. The results are plotted in Fig. 18. It can be observed that there is no significant modification in the shape of the IDI curve due to the multiplexing effect. Moreover, there are no remarkable deviations among the IDI curves related to different CBR load, i.e. the VBR IDI curves related to 100, 110, 120, 130 and 140 Mbps interfering CBR load are almost coincide. On the other hand the correlation structure of the VBR cell stream is given by the IDI curve. For example, the frame structure clearly visible in the Figure. A frame consists of 9 and a half packet with 180 cells as demonstrated in Fig. 15-16. It means that a frame has approximately 1710 cells related to the braking point of the IDI

curve. The highly periodic structure of the video frame, which was demonstrated in Figures 13-16, can also be investigated by the IDI curve, i.e. the decreasing IDI curve shows the negative correlation due to the periodic video frame structure.

6. Conclusion

This paper presents analysis results of experiments investigating traffic characteristics in a real ATM environment. Cell transfer delay and long term cell loss ratio results are reported and analyzed. The statistical multiplexing of a heterogeneous traffic mix and the usage of shaping to gain better link utilization were demonstrated. We can conclude from the analysis results of CBR characteristics that a high rate CBR traffic easily loses the periodic structure and becomes, to some extent, a bursty, partly positively correlated traffic due to multiplexing it with highly bursty VBR traffic. It was shown by several statistical characteristics that the multiplexing can cause significant clumping and dispersion in the CBR traffic which makes difficulties to UPC/NPC and AAL. It was also pointed out that the inherent burstiness of a high rate CBR cell stream, caused by the discrete nature of ATM, plays a dominant part in the total burstiness after the multiplexer. In contrast to the observed remarkable changes in the CBR traffic the correlation structure of the VBR traffic is almost unmodified after the multiplexer. However, the VBR traffic profile has been changed, i.e. the clumping and dispersion phenomena are detectable. The basic periodic structure of the VBR video traffic, which dominantly determines the traffic characteristics, is demonstrated in several time scales.

Acknowledgment

The reported research results are obtained in the joint research program between EUA Ericsson, Telia Research in Sweden and High Speed Networks Lab, Department of Telecommunication and Telematics, Technical University of Budapest in Hungary. The research activity was partly supported by the Board of Hungarian State Eötvös Found.

We would like to thank Lars Westberg and Gunnar Olsson from EUA Ericsson and Alexander Latour-Henner, Urban Hansson and Aziz Miah from Telia Research for the help during the preparation and fulfillment of our measurements.

References

[1] S. Singh, S-S. Chan, "A Multi-Level Approach to the Transport of MPEG-Coded Video Over ATM and Some Experiments"*GLOBECOM'95*, Nov. 13-15, 1995.

[2] J. Pugaczewski, W. Walling, M. Wiklund, "Multimedia Traffic Characterization from the High Definition Distance Learning ATM Trial*", 20th Conference on Local Computer Communications*, Minneapolis, Minesota, Oct. 16-19, 1995.

[3] E. Aarstad, R. Venturin, "Traffic Characterization of the JVTOS Multimedia Application", *The Twelfth Nordic Teletraffic Seminar*, Espoo, Finland, August 22-24, 1995.

[4] H. Haapasalo, I. Norros, T. Raij, "Some Experiments From ATM Traffic Measurements", *The Twelfth Nordic Teletraffic Seminar*, Espoo, Finland, August 22-24, 1995.

[5] G. Karlsson, "Stockholm Gigabit Network", in the Proceedings of the *First IEEE Symposium on Global Data Networking*, Cairo, Egypt, December 12-15, 1993, pp. 7-14.

[6] SunSolutions, Sun Microsystems, Inc., The Complete Guide to ShowMe 2.0.1, June 1994

[7] vic, *FTP://ftp.sunet.se/pub/conference*

[8] ITU-T Rec. I.360., B-ISDN ATM Adaptation Layer (AAL) Functional Description,

[9] ATM Forum, ATM User Network Interface Specification, Version 3.1, September 1994.

[10] ATM Forum, Traffic Management Specification, Version 4.0, April 1996.

[11] ITU-T Recommendation I.356., B-ISDN ATM Layer Cell Transfer Performance

[12] COST 242 “Cell Delay Variation in ATM Networks”, (eds. A. Gravey, S. Blaabjerg), Interim Report, August 1994.

[13] J. Roberts, F. Guillemin, “Jitter in ATM Networks and its Impact on Peak Rate Enforcement”, *Performance Evaluation*, vol. 16, pp. 35-48, 1992.

[14] S. Molnár, S. Blaabjerg and H. Christiansen, “On the Superposition of a Number of CDV Affected Cell Streams”, *International Conference on Local and Metropolitan Communication Systems LAN&MAN*, Kyoto, Japan, Dec. 7-9, 1994.

[15] S. Molnár, S. Blaabjerg “Correlations in ATM Cell Streams Exposed to Cell Delay Variation”, *Journal on Communications*, Vol. 47. January-February, 1996. pp 52-56.

[16] N. Björkman, I. Cselényi, U. Hansson, A. Latour-Henner, A. Miah, “Heuristics for Shaping ATM Traffic from Multimedia Applications”, Internal Report, February 1996

[17] A. Latour-Henner, N. Björkman, I. Cselényi, “Shaping up without delay”, Internal Report, March 1996

[18] O. Melteig, ”Introduction to the PARASOL Project” In *The 9’th Nordic Teletraffic Seminar*, Norwegian Telecom, Research Department, August 21-23, 1990

[19] D.R. Cox, P.A.W. Lewis, ”The Statistical Analysis of Series of Events”, Menthuen, 1966.